



Experimental Data and Modeling of Solid–Liquid Equilibria of Binary Systems Containing Dibenzofuran and Long Chain *n*-alkanes

Issam Boudouh^{1,2} · Baudilio Coto³ · Juan Antonio González⁴ · Irfan Wazeer⁵ · M. Zulhaziman M. Salleh⁶ · Ismahane Djemai⁷ · Maria Dolores Robustillo⁸ · Mohamed K. Hadj-Kali⁵

Received: 24 January 2023 / Accepted: 4 May 2023 / Published online: 4 July 2023

© The Author(s), under exclusive licence to Springer Science+Business Media, LLC, part of Springer Nature 2023

Abstract

Solid–liquid equilibria (SLE) of binary mixtures of several *n*-alkanes (*n*-octadecane, *n*-eicosane, *n*-tetracosane, *n*-pentacosane, *n*-triacontane) and dibenzofuran covering the whole composition range were measured by differential scanning calorimetry (DSC) in a temperature range of 301–356 K. The dibenzofuran and the *n*-alkanes are completely miscible in the liquid state but non-miscible in the solid state, and in the context of this work, they seem to exhibit eutectic behavior. A linear trend is obtained for the eutectic temperature and eutectic composition versus the number of carbon atoms of *n*-alkane. The experimental data were compared to predictions made by using the ideal solution model, the DISQUAC model and several versions of the UNIFAC model, including the classical UNIFAC, the modified versions of Lyngby and Dortmund, and the recently proposed modified UNIFAC (NIST) model, to account for non-ideality in the liquid phase. Moreover, the experimental data were also compared with COSMO-RS predictions that utilize quantum chemical calculations and statistical thermodynamics to interpret the behavior of molecular interactions in the binary mixture. A good agreement was obtained between the predicted and the experimental temperatures.

Keywords DSC · SLE · Long-chain *n*-alkane · Dibenzofuran · UNIFAC · DISQUAC · COSMO-RS

1 Introduction

Solid–liquid equilibria (SLE) are important in chemical and petrochemical development, especially in avoiding problems with flow safety due to solid precipitation during extraction, transportation, and storage of complicated mixtures in liquid reservoirs and heavy oils [1–6]. Polycyclic aromatic hydrocarbons (PAHs) and their derivatives containing oxygen, nitrogen, or sulfur atoms are present in crude oil, heavy oil products from coal, lubricants, or coal tar, and during the chemical conversion of crude oil or the incomplete combustion of hydrocarbon fuels. These chemicals are mutagenic and carcinogenic environmental

pollutants. The assessment of toxicity of PAHs and their derivatives necessitates the consideration of their solubility in various environmental media such as the atmosphere, soil, and water phases. PAHs are a class of organic compounds that exhibit volatility and have the ability to dissolve in atmospheric moisture. These compounds can also form aerosols and vapors, which can be inhaled or deposited on various surfaces. Furthermore, PAHs have the ability to adhere to the surfaces of particles or become physically integrated into particle structures, such as dust, or sediment. The solubility of PAHs in various environmental media plays a crucial role in determining their transport, fate, and bioavailability. This factor can have a considerable impact on the potential of PAHs to cause harm to both human health and the environment [7].

Systems containing polycyclic aromatic and long-chain normal alkanes are considered precursors to the complex systems found in fluid reservoirs. The representation of the thermodynamic properties of these fluids requires the consideration of the binary interactions between the different molecules involved. However, previous studies have been performed on binary mixtures related to the size of these molecules, either from two light components or from an asymmetric combination between heavy and light molecules. Although binary mixtures consisting of straight long-chain alkanes and PAH compounds have been extensively studied in the literature, studies on their thermodynamic properties have been limited. Djordjevic [8] measured the solubilities of five PAHs (naphthalene, acenaphthene, anthracene, phenanthrene, and pyrene) in *n*-octadecane. He concluded that these mixtures are slightly non-ideal, probably due to the compensation between enthalpic and entropic factors.

In addition, the excess free energy curves can be highly asymmetric, resulting in extremely high values for the limiting activity coefficients. For this reason, it is crucial from a practical point of view to have a thorough knowledge of the thermodynamic properties of these systems. Aoulmi et al. [9] investigated the thermodynamics of mixtures consisting of long-chain alkanes and PAHs. The authors investigated the mixing behavior of these compounds in terms of excess entropy of mixing, phase behavior, and heat of mixing while Mahmoud et al. [10] examined the SLE and excess enthalpy of the mixtures formed from long-chain *n*-alkanes and polycyclic heteropolyaromatics. Hafsaoui and Mahmoud [11] measured the SLE for naphthalene + *n*-tetracosane and dibenzofuran + *n*-tetracosane mixtures. A eutectic behavior was observed in these systems. The activity coefficients were obtained by readjusting the interaction parameters of the UNIFAC model.

PAHs are also significant to the refinery sector during hydrocracking because their deposition reduces heat exchange in these units. Aromatic–aromatic interactions stabilize the tertiary structure of proteins, for example and a deeper understanding requires the study of fundamental heteroatomic compounds such as indole, dibenzofuran, and dibenzothiophene [12]. The study of mixtures containing a PAH and a long-chain alkane is essential because they play an important role in the flocculation and deposition of asphaltenes, a very critical issue during the exploitation, transport, and storage of crude oil. The study of these solutions is particularly useful as a starting point for the examination of mixtures containing heteroaromatic molecules, which are abundant in coal tar and coal liquids and are precursors to the complex systems found in fluid reservoirs. However, there are few studies on such binary mixtures in the literature [10, 11, 13–19].

In this work, dibenzofuran was chosen as an example of a polyaromatic compound with a heteroatom and long-chain *n*-alkanes with more than 18 carbon atoms from *n*-octadecane to *n*-triacontane. Understanding the phase behavior of binary systems with dibenzofuran and long-chain *n*-alkanes is important for designing and optimizing separation techniques, which are needed to remove these contaminants from different industrial products and

waste streams. Therefore, the aim of this work is to determine the SLE temperatures by means of differential scanning calorimetry (DSC) for dibenzofuran + *n*-octadecane, dibenzofuran + *n*-eicosane, dibenzofuran + *n*-tetracosane, dibenzofuran + *n*-pentacosane, and dibenzofuran + *n*-triacontane systems. In addition, the experimental results were correlated and compared with predicted values obtained with the ideal solution, UNIFAC [20], and several modifications of the UNIFAC [21–25], DISQUAC [26], and COSMO-RS [27] models to account for the non-ideality of the liquid phase.

2 Experimental Section

2.1 Materials

All chemicals were used as delivered without further purification. The *n*-pentacontane (CAS no. 6596-40-3) and *n*-triacontane (CAS no. 638-68-6) were purchased from Fluka (purity higher than 98%), the *n*-tetracosane (CAS no. 646-31-1) were purchased from Merck (purity higher than 99%), the *n*-eicosane (CAS no. 112-95-8), and dibenzofuran (CAS no. 132-64-9) were obtained from Avocado (purity higher than 99%), and the *n*-octadecane (CAS no. 593-45-3) was purchased from Acros (purity higher than 99%).

2.2 Experimental Procedure

The dibenzofuran and the *n*-alkanes are completely miscible in the liquid state. Experimental methodology was followed as described in the literature [10, 11, 13]; for each binary system, the mixture was heated under constant agitation until complete melting, the sample was heated very slowly inside a glass cell, and the cell was immersed rapidly in a liquid nitrogen bath to obtain a homogeneous solid mixture. A small amount of solid (5 to 10 mg) was sealed in the aluminum pan of the DSC 7 (Perkin-Elmer).

The instrument was calibrated using Indium (purity = 99.99%, $T_m = 429.78$ K, $\Delta H_f = 28.45$ J·g⁻¹). The solubility measurements were conducted under a constant nitrogen flow (20 mL·min⁻¹). The heating rate was fixed at 0.8 °C·min⁻¹. Data acquisition (enthalpy of fusion of the pure compounds and onsets corresponding to the solid–liquid equilibria temperatures) and processing was made with Perkin-Elmer's Pyris software. The measurement uncertainties are estimated to be ± 0.1 K for the temperatures and ± 0.35 kJ·mol⁻¹ for the heat of fusion and solid–solid transition. i.e., the calculated reproducibility of the measurement without disturbance to the system. The calculated reproducibility (repeatability) of the measurement considering external factors such as sample mass, composition, and the fact of removing and replacing the sample in between each run was ± 0.4 K. The uncertainty of the mole fraction is 0.0005. The binary systems (dibenzofuran + *n*-eicosane), (dibenzofuran + *n*-tetracosane), and (dibenzofuran + *n*-pentacosane) have already been studied in the literature [10, 11]. Figures S6 to S8 (Supplementary material) show our values in comparison with those in the literature. The liquidus are very comparable, although our results are slightly higher. This is consistent with the higher melting temperatures of pure substances used during our experiments. It appears that the mean relative deviations on the liquidus temperatures are small. Values of the eutectic heat and of the heat of melting needed to determine the final composition of the eutectic points on the basis of the Tammann plots [14–17] (Figs. S1–S5, Supplementary material) are listed in Table S2, S3, S4, S5, and S6.

3 Model Description

3.1 Determination of Solid–Liquid Phase Diagrams (SLPD)

For the five systems studied in this work, the components are not miscible in the solid phase and exhibit a simple eutectic diagram as the first peak appears at a constant temperature. The equation for the solid–liquid equilibrium is given by

$$\ln(\gamma_i x_i) = -\frac{\Delta H_{m,i}}{RT} \left(1 - \frac{T}{T_{m,i}}\right) + \frac{\Delta C_{p,i}}{R} \left(\ln \frac{T}{T_{m,i}} + \frac{T_{m,i}}{T} - 1\right) - \frac{\Delta H_{tr,i}}{RT} \left(1 - \frac{T}{T_{tr,i}}\right), \quad (1)$$

where $\Delta H_{m,i}$, $T_{m,i}$, $\Delta C_{p,i}$, $\Delta H_{tr,i}$, and $T_{tr,i}$ are respectively the molar enthalpy of melting, the melting temperature, the molar heat capacity change (assumed to be independent of T) during the melting process, the enthalpy change corresponding to the transition, and the transition temperature of the pure component i . To a fair approximation, the term $\Delta C_{p,i}$ in Eq. 1 may be neglected [28]. The last term corresponds to the enthalpic contribution of the first-order transition observed in the solid n -tetracosane, n -pentacosane, and n -triacontane.

According to Eq. 1, SLE data can be used to calculate activity coefficients, γ_i , of the i -component in the mixture from experimental melting temperatures and pure component properties. Otherwise, when activity coefficients are calculated from a predictive model for the liquid phase, Eq. 1 can be used to predict the melting temperature for a given mixture.

3.2 UNIFAC Model

According to the UNIFAC model [20], Modified UNIFAC (Lyngby) by Larsen et al. [23, 24], Modified UNIFAC (Dortmund) by Gmehling et al. [21–23], and Modified UNIFAC (NIST) by Kang et al. [25], activity coefficient γ_i of component i in the liquid phase is given by

$$\ln(\gamma_i) = \ln(\gamma_i)^C + \ln(\gamma_i)^R, \quad (2)$$

$$\ln(\gamma_i)^C = 1 - \frac{w'_i}{x_i} + \ln\left(\frac{w'_i}{x_i}\right) - 5q_i \left(1 - \frac{w_i}{\theta_i} + \ln\left(\frac{w_i}{\theta_i}\right)\right), \quad (3)$$

$$w_i = \frac{x_i r_i}{\sum_j x_j r_j}; w'_i = \frac{x_i r_i^\alpha}{\sum_j x_j r_j^\alpha}; \theta_i = \frac{x_i q_i}{\sum_j x_j q_j}. \quad (4)$$

For components i , r_i and q_i are the volume and surface structural parameters, respectively, w_i and w'_i are volume fractions, and θ_i is the surface fraction.

$$\ln(\gamma_i)^R = \sum_k v_k^{(i)} (\ln \Gamma_k - \ln \Gamma_k^{(i)}), \quad (5)$$

$$\ln \Gamma_k = \frac{z}{2} Q_k \left[1 - \ln \left(\sum_m \Theta_m \Psi_{mk} \right) - \sum_m \frac{\Theta_m \Psi_{km}}{\sum_n \Theta_n \Psi_{nm}} \right], \quad (6)$$

where $v_k^{(i)}$ is the number of groups k in the molecule i , Γ_k is the group activity coefficient in the mixture, $\Gamma_k^{(i)}$ is the group activity coefficient of group k in pure i , z is the coordination number equal to 10, Q_k and θ_k are the surface structural parameter and the surface fraction of group k , Ψ_{nm} contains the interaction parameters:

$$\Psi_{nm} = \exp \left[-\frac{a_{nm}}{T} \right]. \quad (7)$$

In the original UNIFAC version, $\alpha=1$ and the UNIFAC group interaction parameters between groups n and m , a_{nm} , are assumed to be temperature independent.

3.3 Modified UNIFAC Model (Lyngby Version)

In Modified UNIFAC (Lyngby) by Larsen et al. [23, 24], combinatorial contribution given by Eq. 3 is replaced by

$$\ln(\gamma_i)^C = 1 - \frac{w'_i}{x_i} + \ln \left(\frac{w'_i}{x_i} \right), \quad (3')$$

where $\alpha=2/3$ in w'_i and Ψ_{nm} is given by

$$\Psi_{nm} = \exp \left[-\frac{a_{nm,1} + a_{nm,2}(T - T_0) + a_{nm,3} \left(T \ln \frac{T_0}{T} + T - T_0 \right)}{T} \right], \quad (7')$$

where T_0 is a reference temperature set equal to 298 K and the interaction between groups n and m is given by the three parameters $a_{nm,1}$, $a_{nm,2}$, and $a_{nm,3}$ to improve the temperature effect.

3.4 Modified UNIFAC Model (Dortmund Version)

In the Modified UNIFAC (Dortmund) by Gmehling et al. version [21–23], $\alpha=3/4$ in w'_i and Ψ_{nm} is given by

$$\Psi_{nm} = \exp \left[-\frac{a_{nm,1} + a_{nm,2}T + a_{nm,3}T^2}{T} \right], \quad (7'')$$

where interaction between groups n and m is given by parameters $a_{nm,1}$, $a_{nm,2}$, and $a_{nm,3}$.

3.5 New Modified UNIFAC Model (NIST Version)

In the New Modified UNIFAC by Kang et al. version [25], $\alpha=3/4$ in w'_i and Ψ_{nm} is identical to Eq 7''. This version included the specific group "furan" for describing cyclic ethers as dibenzofuran.

Structural parameters, R and Q , and interaction parameters for the several UNIFAC model versions for the ether group are listed in Table 1.

3.6 DISQUAC Model

Some important features of the model are the following. (i) DISQUAC is a group contribution model based on the rigid lattice theory developed by Guggenheim. [29] (ii) The total molecular volumes, r_i , surfaces, q_i , and the molecular surface fractions, α_i , of the compounds present in the mixture, are calculated additively based on the group volumes R_G and surfaces Q_G recommended by Bondi [30] (see below). (iii) The

Table 1 Structural and interaction parameters for ether group involved in the dibenzofuran + *n*-alkane systems

	UNIFAC	Mod.UNIFAC (Lyngby)	Mod.UNIFAC (Dortmund)	Mod.UNIFAC (NIST)
R (ether)	0.6908	0.6908	1.1434	
Q (ether)	0.4680	0.6500	0.8968	
R (furan)			0.9743	0.9743
Q (furan)			0.4800	0.4800
a (CH ₂ -ACH)	61.13	62.88 −0.2493 1.103	114.2 0.0933 −	137.14 −0.32 1.25e-3
a (ACH-CH ₂)	−11.12	−1.447 −0.5638 −1.612	16.070 −0.2998 −	65.28 −0.4342 −0.194e-3
a (CH ₂ -ether)	251.5	230.5 −1.328 −2.476	233.1 −0.3155 −	
a (ether-CH ₂)	83.36	369.9 −1.542 −3.228	−9.654 −0.03242 −	
a (CH ₂ -furan)				−17.57 − −
a (furan-CH ₂)				167.46 − −
a (ACH-ether)	32.14	82.86 0.6106 −0.7392	−87.08 −0.1859 −	
a (ether-ACH)	52.13	125.2 −1.093 0.5898	179.0 0.05615 −	
a (ACH-furan)				277.97 − −
a (furan-ACH)				−136.73 − −

partition function is factorized into two terms, in such a way that the excess functions are calculated as the sum of two contributions: a dispersive (DIS) term, which represents the contribution from the dispersive forces; and a quasichemical (QUAC) term which arises from the anisotropy of the field forces created by the solution molecules. In the case of the Gibbs energy, G_m^E a combinatorial term $G_m^{E,COMB}$ represented by the Flory–Huggins equation [31, 32] must be considered. Thus,

$$G_m^E = G_m^{E,COMB} + G_m^{E,DIS} + G_m^{E,QUAC}, \quad (8)$$

$$H_m^E = H_m^{E,DIS} + H_m^{E,QUAC}. \quad (9)$$

(iv) The interaction parameters depend on the molecular structure; (v) the value $z=4$ for the coordination number is used for all the polar contacts. This represents one of the more important shortcomings of the model and is partially removed via the hypothesis of considering structure-dependent interaction parameters. (vi) The equations used to calculate the DIS and QUAC contributions to G_m^E and H_m^E in the framework of DISQUAC are given elsewhere [33]. The temperature dependence of the interaction parameters, $g_{st}^{DIS/QUAC}$ (Gibbs energy); $h_{st}^{DIS/QUAC}$ (enthalpy) and $c_{pst}^{DIS/QUAC}$ (heat capacity) is expressed in terms of the DIS and QUAC interchange coefficients [33] $C_{st,l}^{DIS}$; $C_{st,l}^{QUAC}$ where $s \neq t$ are two contact surfaces present in the mixture and $l = 1$ (Gibbs energy); $l = 2$ (enthalpy), $l = 3$ (heat capacity). The needed equations are [33]

$$\frac{g_{st}^{DIS/QUAC}}{RT} = C_{st,1}^{DIS/QUAC} + C_{st,2}^{DIS/QUAC} \left[\frac{T_0}{T} - 1 \right] + C_{st,3}^{DIS/QUAC} \left[\ln\left(\frac{T_0}{T}\right) - \frac{T_0}{T} + 1 \right], \quad (10)$$

$$\frac{h_{st}^{DIS/QUAC}}{RT} = C_{st,2}^{DIS/QUAC} \frac{T_0}{T} - C_{st,3}^{DIS/QUAC} \left(\frac{T_0}{T} - 1 \right), \quad (11)$$

$$\frac{c_{pst}^{DIS/QUAC}}{R} = C_{st,3}^{DIS/QUAC}. \quad (12)$$

(vii) Dibenzofuran + *n*-alkane mixtures are built by three surfaces (groups): type a, aliphatic (CH₃, CH₂), in *n*-alkanes; type b, aromatic in dibenzofuran, and type e, oxygen (-O- in dibenzofuran). The geometrical parameters of the groups referred to in this work are available in the literature [14]. For dibenzofuran, $r = 5.2766$, $q = 3.4140$, $\alpha_b = 0.9399$, $\alpha_e = 0.0606$. (viii) These surfaces generate three contacts: (a,b); (a,e); and (b,e). The (a,b) contact is characterized by purely dispersive interaction parameters equal to those of naphthalene + *n*-alkane mixtures [34]. Interactions parameters for the (a,e) and (b,e) contacts are represented by DIS and QUAC interchange coefficients. The fitting procedure has been explained in detail elsewhere [33]. We remark that, due to the necessary experimental data, the QUAC interaction parameters used for the (a,e) and (b,e) contacts are those reported for aromatic ether + alkane systems [35]. Table 2 shows our values of the interaction parameters for the mentioned contacts. The geometrical parameters for the groups referred to in this work are listed in Table S1 (Supplementary Material).

Table 2 Dispersive (DIS) and quasichemical (QUAC) interchange coefficients, $C_{st,l}^{DIS}$ and $C_{st,l}^{QUAC}$ ($l=1$, Gibbs energy; $l=2$, enthalpy; $l=3$, heat capacity) for (s,e) contacts^a dibenzofuran + *n*-alkane mixtures

Contact ^a	$C_{st,1}^{DIS}$	$C_{st,2}^{DIS}$	$C_{st,3}^{DIS}$	$C_{st,1}^{QUAC}$	$C_{st,2}^{QUAC}$	$C_{st,3}^{QUAC}$
(a, e)	39.2	27.5	15	− 0.5	− 1	20
(b, e)	34.5	27.33		6	12	

^atype a, aliphatic in *n*-alkanes, type b, aromatic in dibenzofuran, type e, oxygen in dibenzofuran

3.7 COSMO-RS Model

The Conductor-like Screening Model for Real Solvents (COSMO-RS) was used to predict and compare the solid–liquid phase equilibria of dibenzofuran + *n*-alkanes [27, 36]. The geometry optimization of the organic compound (dibenzofuran) and the *n*-alkanes (*n*-octadecane, *n*-eicosane, *n*-tetracosane, *n*-pentacosane, and *n*-tricosane) was performed using the Turbomole program package. The chemical structure of the target molecule was firstly drawn in three dimensional. Afterward, geometry optimization was performed at the Hartree–Fock level and 6-31G* basis set. In this work, only the lowest energy conformer was considered for the COSMO-RS calculation. During the optimization, the positions of atoms in the molecule were adjusted to find the lowest energy conformation of the molecule. This involved changing the three-dimensional coordinates of the atoms by varying the structural factors such as bond lengths, bond angles, bond rotations, and dihedral (torsional) angles. The generation of the.cosmo file was conducted through a single-point calculation using DFT with Becke–Perdew and the Triple- ζ Zeta Valence Potential (TZVP) basis set. Finally, the.cosmo files were exported to the COSMOthermX program of version 19.0.5, with parameterization BP_TZVP_19.ctd.

COSMO-RS is a computational model which combines two methods, i.e., (i) quantum chemical considerations in the form of a conductor-like-screening tool and (ii) statistical thermodynamics. This enables the determination and prediction of thermodynamic properties without requiring experimental data. In this work, COSMO-RS was used to compute a range of binary concentrations for dibenzofuran + *n*-alkanes at which the solidification occurs. The comparison between COSMO-RS prediction data can be compared visually in phase equilibria involved in this study.

The following equation calculates the chemical potential of the surface segments:

$$\mu_S(\delta) = -\frac{RT}{\alpha_{\text{eff}}} \ln \left[\int \rho_S(\delta') \exp \left(\frac{1}{RT(\alpha_{\text{eff}}\mu_S(\delta') - E_{\text{misfit}}(\delta, \delta') - E_{\text{hb}}(\delta, \delta'))} \right) \right]. \quad (13)$$

This set of COSMO-RS equations gives the chemical potential of all components in a mixture, which enables the estimation of several thermodynamic properties, such as activity coefficients, selectivities, distribution ratios, and phase equilibria. The detailed derivations have been described by the developers elsewhere [37–39], where the main resulting equations applied in COSMO-RS and their constants are summarized in Table 3.

In this work, when applying the COSMO-RS model, the second and the third terms in Eq. 1 were neglected (both the difference between the molar heat capacity of the solid and the subcooled liquid form and the enthalpic contribution of the first-order transition, respectively) yielding to the simplified equation:

Table 3 Equations and constants in COSMO-RS model

Measurement	Mathematical expressions
Electrostatic misfit energy	$E_{\text{misfit}}(\sigma, \sigma') = \alpha_{\text{eff}}' \frac{\alpha'}{2} (\sigma + \sigma')^2$
Hydrogen Bond interaction energy	$E_{\text{hb}} = \alpha_{\text{eff}} c_{\text{hb}} \min(0, \sigma \sigma' + \sigma_{\text{hb}}^2)$
Van Der Waals interaction energy	$E_{\text{vdw}} = \alpha_{\text{eff}} (\tau_{\text{vdw}} + \tau'_{\text{vdw}})$
Chemical potential of a segment	$\mu_s(\sigma) = -RT \ln \left[\int d\sigma' p_s(\sigma) \times \exp \left\{ -\frac{1}{2} \alpha' (\alpha + \alpha')^2 - \mu_s(\sigma') / RT \right\} \right]$
Activity coefficient of a segment	$\ln \gamma_s(\sigma) = -\ln \left[\int d\sigma' p_s(\sigma) \gamma_s(\sigma') \times \exp \left\{ \frac{-\alpha_{\text{eff}}(\sigma, \sigma')}{RT} \right\} \right]$
Activity coefficient of a solute <i>i</i> in an ensemble <i>S</i>	$\ln \gamma_{i/S}(\sigma) = \ln \gamma_{i/S}^{\text{res}} + \ln \gamma_{i/S}^{\text{comb}}$
Residual activity coefficient	$\ln \gamma_{i/S}^{\text{res}}(\sigma) = -n_i \left[\int d\sigma' p_i(\sigma) \{ \ln \gamma_s(\sigma') - \gamma_i(\sigma') \} \right] + \ln \gamma_{i/S}^{\text{comb}}$
Combinatorial activity coefficient	$\ln \gamma_{i/S}^{\text{comb}} = \ln \frac{\phi_i}{x_i} + \frac{z}{2} q_i \ln \frac{\theta_i}{\phi_i} + l_i - \frac{\phi_i}{x_i} \sum x_j l_j$ $\theta_i = \frac{x_i q_i}{\sum_j x_j q_j}$ $\theta_i = \frac{x_i r_i}{\sum_j x_j r_j}$ $l_i = \frac{z}{2} ((r_i - q_i) - (r_i - 1))$
σ -profile of a mixture	$p_s(\sigma) = \sum_{i \in S} x_i p^s(\sigma)$
Constants	
α'	General constant
α_{eff}	Effective contact area
c_{hb}	Interaction strength coefficient
σ_{hb}	Polarization charge density threshold for hydrogen bond
τ_{vdw}	Element-specific parameter for dispersion coefficient

$$\ln(x_i) = -\ln(\gamma_i) - \frac{\Delta H_{m,i}}{RT} \left(1 - \frac{T}{T_{m,i}} \right). \quad (14)$$

So, the only input data for the COSMO-RS model are the enthalpy of fusion (ΔH_m) and the melting point temperature (T_m) for each pure species manually assigned according to the data reported in Table 4.

4 Results and Discussion

The DSC heating thermograms corresponding to binary mixtures show two peaks. The onset temperature of the first peak (the one observed at the lowest temperature) is independent of the concentration and corresponds to the eutectic transition, while the second one is concentration dependent, and its onset temperature corresponds to the liquidus temperature. At the eutectic composition, the thermogram only presents a peak whose shape is similar to that of the pure compounds.

Phase change properties of the pure compounds are reported in Table 4, together with the values from the literature. These properties are globally in fair agreement with literature data [10, 11, 13, 40–44]. The experimental data obtained for the SLE determination of dibenzofuran with *n*-alkane systems are listed in Table 5.

Table 5 lists experimental data obtained for the SLE determination of dibenzofuran with *n*-alkane systems. *n*-alkane range from *n*-octadecane up to *n*-triacontane and covered temperature range was 301–356 K. Eutectic points are determined, and they are

Table 4 Thermodynamic properties of the studied pure substances

Compound	T_m /K	ΔH_m /kJ·mol ⁻¹	T_f /K	ΔH_f /kJ·mol ⁻¹
dibenzofuran	355.45 ^a	18.50 ^a	–	–
	355.20 ^c	18.60 ^c	–	–
<i>n</i> -octadecane	300.32 ^a	65.33 ^a	–	–
	300.40 ^b	61.70 ^b	–	–
	301.10 ⁱ	60.10 ⁱ	–	–
<i>n</i> -eicosane	309.93 ^a	67.45 ^a	–	–
	310.00 ^c	69.88 ^c	–	–
	311.60 ^e	69.03 ^e	–	–
	309.70 ⁱ	68.10 ⁱ	–	–
<i>n</i> -tetracosane	324.18 ^a	49.60 ^a	321.49 ^a	27.39 ^a
	324.45 ^f	55.51 ^f	320.38 ^f	31.18 ^f
	323.75 ^d	54.84 ^d	321.25 ^d	31.27 ^d
	324.10 ^h	59.30 ^h	321.03 ^h	33.18 ^h
<i>n</i> -pentacosane	327.12 ^a	51.23 ^a	318.75 ^a	27.34 ^a
	326.00 ^c	54.04 ^c	319.30 ^c	24.43 ^c
	325.92 ^e	55.53 ^e	309.00 ^e ; 312.90 ^e	23.90 ^e ; 1.07 ^e
<i>n</i> -triacontane	338.04 ^a	70.13 ^a	331.22 ^a	36.47 ^a
	338.11 ^b	67.07 ^b	–	–
	–	–	335.25 ^g	37.49 ^g

^aThis work, ^b[13], ^c[10], ^d[40], ^e[41], ^f[42], ^g[43], ^h[11], ⁱ[44]

marked in Table 5 by $T_{m(1)}^*$ and x_1^* . Activity coefficient values calculated from Eq. 1 are also listed. As shown in Table 5, the experimental values of $T_{m(1)}^*$ and x_1^* , corresponding to the eutectic points depend on the chain length of *n*-alkane and increase with the increase of the number of carbon atoms.

Figure 1 represents the eutectic coordinates, composition, and temperature versus the number of carbon atoms for *n*-alkane, and a straight forward linear trend can be found for both magnitudes.

The objective of this study was a better understanding of the thermodynamic properties of mixtures formed by dibenzofuran and one long-chain *n*-alkane hydrocarbon. Calculated values were performed with ideal solution, classical UNIFAC [18], and modified UNIFAC versions of Lyngby [23, 24], Dortmund [21–23], and NIST [25] models, with the parameters from Table 1.

Predicted melting temperatures were compared with those obtained experimentally by using DSC in terms of the mean percent relative deviation, σ_T (%), as defined in Eq. 15:

$$\sigma_T(\%) = \left[\frac{1}{n} \sum_j \left(\frac{T_{\text{exp}}^j - T_{\text{cal}}^j}{T_{\text{exp}}^j} \right)^2 \right]^{1/2} \cdot 100, \quad (15)$$

where n is the number of experimental data points, and subscripts exp and cal stand for experimental and calculated values. Values obtained for each studied system and the whole experimental data collection are reported in Table 6.

Table 5 SLE of dibenzofuran in solution with *n*-alkanes

x_1	$T_{m(1)}/\text{K}$	$T_{m(2)}/\text{K}$	$\gamma_{(1)}$	$\gamma_{(2)}$
Dibenzofuran (1) + <i>n</i> -C18 (2)				
0.0000	300.3			1.0000
0.0916	300.1			1.0771
0.1725*	299.3*			1.1005
0.2779		323.8	1.9496	
0.3611		328.6	1.6599	
0.4559		334.0	1.4659	
0.5409		339.6	1.3807	
0.6352		344.1	1.2801	
0.7250		346.7	1.1773	
0.8099		349.7	1.1134	
0.9089		352.6	1.0450	
1.0000		355.5	1.0000	
Dibenzofuran (1) + <i>n</i> -C20 (2)				
0.0000	309.9			1.0000
0.0750	309.7			1.0603
0.1985*	306.3*			0.9110
0.2899		320.8	1.7525	
0.3385		329.0	1.7861	
0.4981		334.8	1.3633	
0.6127		340.3	1.2352	
0.7115		343.6	1.1315	
0.7961		346.9	1.0765	
0.8947		350.3	1.0185	
1.0000		355.5	1.0000	
Dibenzofuran (1) + <i>n</i> -C24 (2)				
0.0000	324.2			1.0000
0.0948	321.9			0.9670
0.1949	320.4			0.9968
0.3075*	319.0*			1.0679
0.4009		324.2	1.3629	
0.5005		330.3	1.2405	
0.6055		336.9	1.1689	
0.6879		341.3	1.1204	
0.7957		347.0	1.0781	
0.8895		351.4	1.0450	
1.0000		355.5	1.0000	
Dibenzofuran (1) + <i>n</i> -C25 (2)				
0.0000	327.1			1.0000
0.1085	326.6			1.0854
0.1895	325.2			1.1040
0.2975	323.6			1.1564
0.3519*	321.7*			1.1201
0.4475		329.9	1.3756	
0.5001		333.5	1.3231	
0.5979		339.3	1.2404	

Table 5 (continued)

x_1	$T_{m(1)}/\text{K}$	$T_{m(2)}/\text{K}$	$\gamma_{(1)}$	$\gamma_{(2)}$
0.6988		343.5	1.1510	
0.7941		347.7	1.0943	
0.9005		351.5	1.0341	
1.0000		355.5	1.0000	
Dibenzofuran (1) + <i>n</i> -C30 (2)				
0.0000	338.0			1.0000
0.0985	337.1			1.0309
0.1995	336.3			1.0939
0.2975	335.6			1.1829
0.3985	334.5			1.2719
0.5045*	333.9*			1.4756
0.6095		339.8	1.2286	
0.6995		343.9	1.1575	
0.7975		347.8	1.0916	
0.8985		351.4	1.0346	
1.0000		355.5	1.0000	

Standard uncertainties are: $U(P)=0.2$ kPa; $U(\times 1)=0.0005$, and the combined expanded uncertainty (0.95 level of confidence) for temperature is $UC(T)=0.4$ K

*Corresponding to the eutectic point

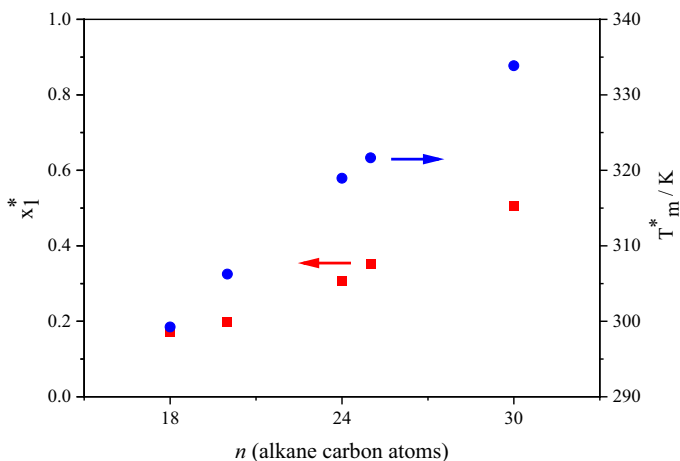
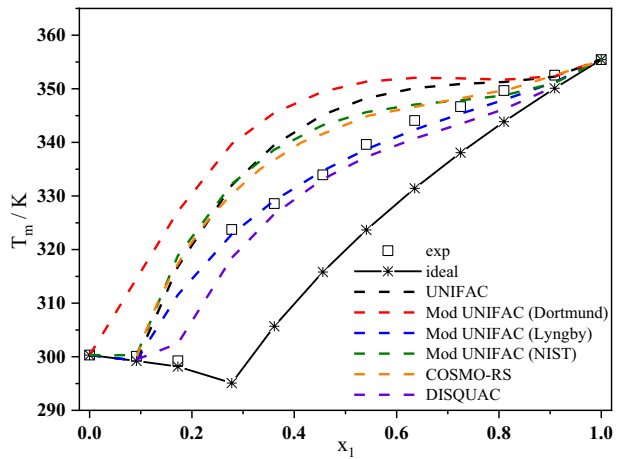
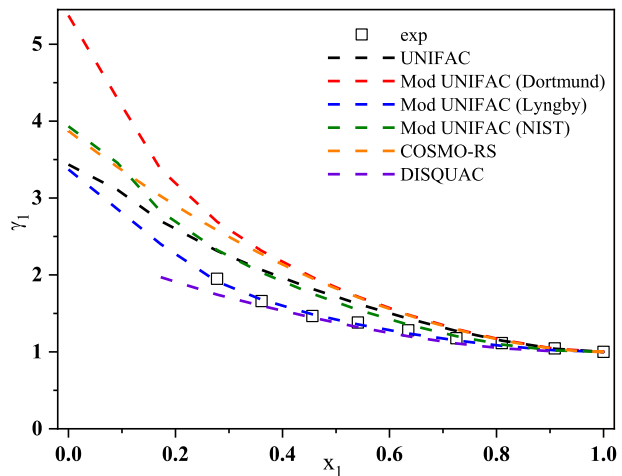


Fig. 1 Experimental eutectic composition (Filled circle) and eutectic melting temperature (Filled Square) of binary mixtures dibenzofuran + *n*-alkane versus the alkane number of carbon atoms

Figure 2 plots melting temperature versus mole fraction, and Fig. 3 plots the dibenzofuran activity coefficient for the system Dibenzofuran (1) + *n*-C18 (2); experimental and calculated values are plotted together. As expected, the ideal solution results in a clear underestimation of melting temperatures and composition for the eutectic point higher than the experimental value. Most UNIFAC model versions change such descriptions

Table 6 Mean percent deviations in precipitation temperature resulting from calculations using UNIFAC versions, DISQUAC, and COSMO-RS model

System	Ideal	UNIFAC	Mod. UNIFAC (Lyngby)	Mod. UNIFAC (Dortmund)	Mod. UNIFAC (NIST)	DISQUAC	COSMO-RS
	σ_T (%)	σ_T (%)	σ_T (%)	σ_T (%)	σ_T (%)	σ_T (%)	σ_T (%)
Dibenzofuran (1)							
+ <i>n</i> -C18 (2)	4.01	2.49	1.23	3.97	2.43	0.87	1.52
+ <i>n</i> -C20 (2)	3.01	2.44	0.92	3.71	2.24	1.60	2.55
+ <i>n</i> -C24 (2)	1.50	2.97	1.31	3.99	2.61	0.43	3.36
+ <i>n</i> -C25 (2)	2.02	2.69	0.98	3.81	2.34	0.53	2.45
+ <i>n</i> -C30 (2)	1.29	1.91	0.69	2.62	1.50	0.79	1.75
All systems	2.58	2.53	1.05	3.66	2.26	0.90	2.31

Fig. 2 Experimental and predicted melting temperatures for binary mixture dibenzofuran + *n*-C18 covering the whole composition range. Predictions for the several UNIFAC versions were carried out with parameters from Table 1**Fig. 3** Experimental dibenzofuran activity coefficients for binary mixtures dibenzofuran + *n*-C18 and studied models. Predictions for the several UNIFAC versions were carried out with parameters from Table 1

and overestimate the deviations from ideal behavior, as shown in Fig. 3. Thus, they yield melting temperatures higher than experimental ones and shift the calculated eutectic composition to lower values. Similar plots and analyses could be obtained for the other binary systems studied. Calculated deviations from Table 6 show that the overall value for ideal solution, 2.58%, is similar to those obtained for UNIFAC model versions except for the Lyngby model, which yields the best results with a global deviation of around 1%, as it could also be seen in Fig. 2.

A similar comparison can be carried out for the activity coefficient values. Equation 16 gives the expression for the average standard deviation (%) between activity coefficients for each component calculated by the thermodynamic model and those obtained experimentally and listed in Table 5:

$$\sigma_{\gamma(i)}(\%) = \left[\frac{1}{n} \sum_j \left(\frac{\gamma_{i,\text{exp}}^j - \gamma_{i,\text{cal}}^j}{\gamma_{i,\text{exp}}^j} \right)^2 \right]^{1/2} \cdot 100 \quad i = 1, 2. \quad (16)$$

Table 7 lists obtained values for the several models considered. As can be checked, the deviations in the activity coefficients are usually very high, mainly for component 1, despite the reasonably good deviations obtained for the melting temperatures. The obtained deviations showed that the application of this model with original interaction parameters could not reproduce a good behavior for the studied systems.

It was possible to represent better all systems studied by a readjustment of some of the UNIFAC interaction parameter models. Binary interaction parameter values between the aliphatic group with both aromatic and ether groups were assumed to have the main effect in these systems, according to S. L. Hafsouli and R. Mahmoud [11]. Alternative parameter values for both versions of the modified UNIFAC model were taken from [11], and values for the UNIFAC model were obtained in the present work. Parameter optimization was carried out by minimizing the sum of the two objective functions defined as follows:

$$F_{01} = \left[\frac{1}{n} \sum_j \left(\frac{\gamma_{1,\text{exp}}^j - \gamma_{1,\text{cal}}^j}{\gamma_{1,\text{exp}}^j} \right) \right]; F_{02} = \left[\frac{1}{n} \sum_j \left(\frac{\gamma_{2,\text{exp}}^j - \gamma_{2,\text{cal}}^j}{\gamma_{2,\text{exp}}^j} \right) \right]. \quad (17)$$

F_{01} and F_{02} indicate the objective function representing the part rich in dibenzofuran and that rich in *n*-alkane. Alternative values for interaction parameters are listed in Table 8.

Predicted melting temperatures and predicted activity coefficient values with these alternative parameters were compared with those obtained experimentally in terms of the mean percent relative deviation, $\sigma(\%)$, as defined in Eqs. 15 and 16, respectively. Accepted values are listed in Tables 9 and 10. The modified UNIFAC (Lyngby) does not improve the description and leads to an overall deviation of $\sigma_T = 1.21\%$, similar to the original model versions. However, the modified UNIFAC (Dortmund) version, even when given the least accurate description, $\sigma_T = 1.56\%$, represents a significant improvement from the original parameters. A better description is obtained with the original UNIFAC and the modified UNIFAC (Lyngby) with the furan group, with deviations ranging from 0.6 to 0.7%. Similar conclusions could be obtained when the comparison takes into account the deviations in activity coefficients (Table 10). Compared with

Table 7 Mean percent deviations in activity coefficients resulting from calculations using three UNIFAC versions with original parameters from Table 1, DISQUAC, and COSMO-RS model

	UNIFAC		Mod.UNIFAC (Lyn- gby)		Mod.UNIFAC (Dort- mund)		Mod.UNIFAC (NIST)		DISQUAC		COSMO-RS	
	σ_1 (%)	σ_2 (%)	σ_1 (%)	σ_2 (%)	σ_1 (%)	σ_2 (%)	σ_1 (%)	σ_2 (%)	σ_1 (%)	σ_2 (%)	σ_1 (%)	σ_2 (%)
Dibenzofuran (1)												
+ <i>n</i> -C18 (2)	15.09	5.76	2.14	5.89	23.92	5.39	12.69	5.55	5.80	6.80	22.91	5.48
+ <i>n</i> -C20 (2)	17.11	7.70	3.56	7.49	25.85	8.19	14.28	7.98	11.4	8.90	28.32	8.20
+ <i>n</i> -C24 (2)	25.82	2.35	10.80	2.56	35.82	2.36	22.59	2.28	2.20	4.20	40.99	2.44
+ <i>n</i> -C25 (2)	25.52	7.25	8.34	7.79	33.42	6.29	20.13	6.68	6.80	18.7	35.41	5.86
+ <i>n</i> -C30 (2)	17.29	13.79	5.52	15.11	23.68	11.66	13.34	12.45	5.60	17.1	27.10	9.46
All systems	20.24	9.01	6.86	9.69	29.10	7.94	17.16	8.33	6.36	11.14	31.34	6.98

Table 8 Alternative interaction parameters for ether group involved in the dibenzofuran + *n*-alkane systems

	UNIFAC	Mod.UNIFAC (Lyngby)	Mod.UNIFAC (Dortmund)
<i>a</i> (CH ₂ -ACH)	22.9 ^a	68.16 ^b	41.27 ^b
<i>a</i> (CH ₂ -ether)	221.1 ^a	173.37 ^b	156.15 ^b
<i>a</i> (CH ₂ -furan)		180.0 ^a	
<i>a</i> (furan-CH ₂)		330.0 ^a	
<i>a</i> (ACH-furan)		82.8 ^a	
<i>a</i> (furan-ACH)		125.2 ^a	

^aThis work^bFrom reference [11], values for a_{nm} , 1 in Eqs. 7' and 7''**Table 9** Mean percent deviations in precipitation temperature resulting from calculations using three UNIFAC versions with modified parameters (Table 8) and the DISQUAC model

System	Ideal	UNIFAC	Mod.UNIFAC (Lyngby) ^a	Mod.UNIFAC (Lyngby) ^b	Mod.UNIFAC (Dortmund)	DISQUAC
	σ_T (%)	σ_T (%)	σ_T (%)	σ_T (%)	σ_T (%)	σ_T (%)
Dibenzofuran (1)						
+ <i>n</i> -C18 (2)	4.01	0.67	1.19	1.00	2.22	0.87
+ <i>n</i> -C20 (2)	3.01	0.70	1.01	0.56	1.98	1.60
+ <i>n</i> -C24 (2)	1.50	0.77	1.57	0.77	0.83	0.43
+ <i>n</i> -C25 (2)	2.02	0.42	1.25	0.50	1.28	0.53
+ <i>n</i> -C30 (2)	1.29	0.42	0.93	0.42	1.00	0.79
All systems	2.58	0.62	1.21	0.69	1.56	0.90

^aOriginal ether group^bFuran group as defined in Mod UNIFAC (NIST) model

results provided by the other models, DISQUAC results are slightly better than those obtained from the UNIFAC models using original interaction parameters. In contrast, calculations from Dortmund UNIFAC with new interaction parameters slightly improve DISQUAC results.

Figures 4 and 5 plot the experimental and predicted values for the eutectic melting temperature and eutectic composition. The linear trend previously described in Fig. 1 is correctly described; however, deviations in eutectic composition are more significant than deviations in eutectic melting temperature, as expected from the low percent deviations obtained for melting temperatures.

The interactions between dibenzofuran and *n*-alkanes molecules can explain the solid–liquid phase equilibria based on the σ -profile and σ -potential. Its developers have demonstrated the validity of this approach in detail and reported in several recent studies involving molecular interactions analysis [37, 38]. In the σ -profile, when the screening charge density exceeds $\pm 0.0084 \text{ e\AA}^{-2}$, the molecule is considered adequately polar to induce hydrogen bonding. A higher absolute value of σ leads to a compound being a stronger hydrogen bond donor or hydrogen bond acceptor. For the horizontal axis, increasing negative and positive values for the hydrogen bonding threshold ($\pm 0.0084 \text{ e\AA}^{-2}$)

Table 10 Mean percent deviations resulting from calculations using three UNIFAC versions with modified parameters (Table 8) and from DISQUAC application using the parameters listed in Table 2

	UNIFAC		Mod.UNIFAC (Lyngby) ^a		Mod.UNIFAC (Lyngby) ^b		Mod.UNIFAC (Dortmund)		DISQUAC	
	σ_{T_1} (%)	σ_{T_2} (%)	σ_{T_1} (%)	σ_{T_2} (%)	σ_{T_1} (%)	σ_{T_2} (%)	σ_{T_1} (%)	σ_{T_2} (%)	σ_{T_1} (%)	σ_{T_2} (%)
Dibenzofuran (1)										
+ <i>n</i> -C18 (2)	4.93	6.13	2.08	5.93	5.38	6.05	15.73	6.32	5.80	6.80
+ <i>n</i> -C20 (2)	5.21	7.18	5.00	7.46	3.31	7.30	14.09	6.89	11.4	8.90
+ <i>n</i> -C24 (2)	6.22	2.86	13.02	2.55	6.19	2.72	10.37	3.36	2.20	4.20
+ <i>n</i> -C25 (2)	2.64	8.45	10.66	7.76	3.65	8.17	12.15	9.26	6.80	18.7
+ <i>n</i> -C30 (2)	2.16	16.33	8.00	14.82	2.38	15.77	9.80	17.96	5.60	17.1
All systems	4.63	10.37	8.66	9.55	4.50	10.06	12.76	11.28	6.36	11.14

^aOriginal ether group^bFuran group as defined in Mod UNIFAC (NIST) model

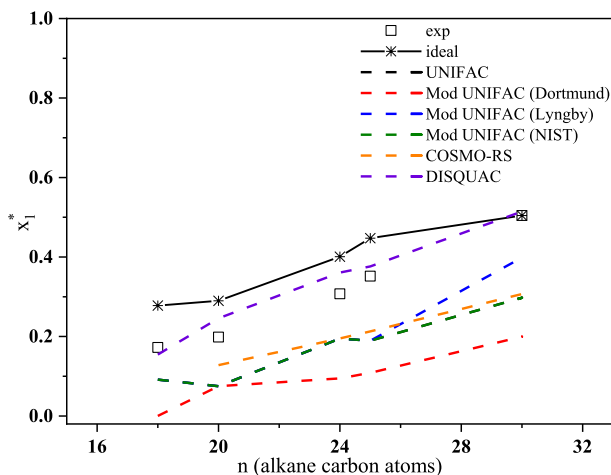
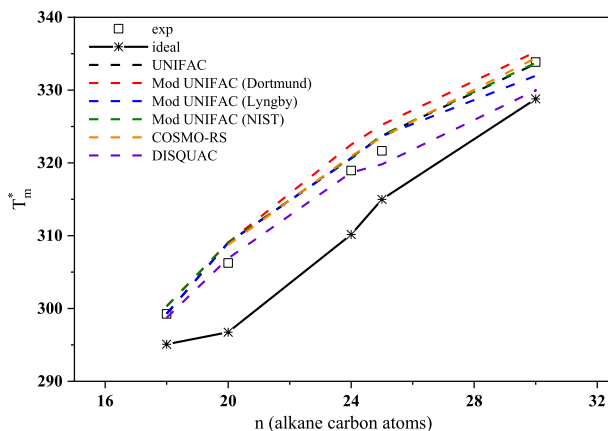


Fig. 4 Experimental eutectic composition of binary mixtures dibenzofuran + *n*-alkane and studied models versus the alkane number of carbon atoms

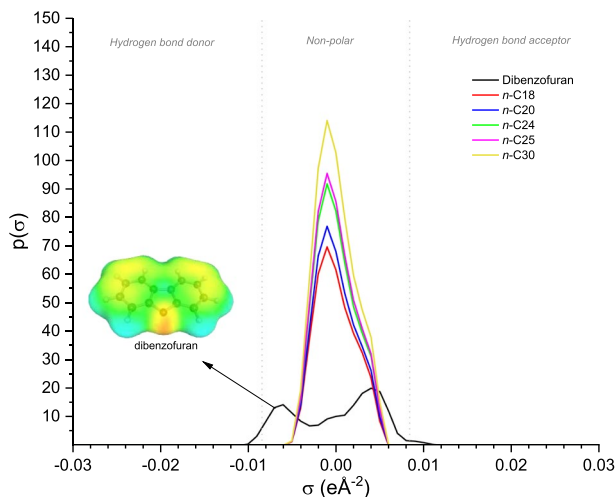
Fig. 5 Experimental eutectic melting temperatures of binary mixtures dibenzofuran + *n*-alkane and studied models versus the alkane number of carbon atoms



indicates the region of a molecule where interactions between hydrogen bond donors and hydrogen bond acceptors occur, respectively.

On the other hand, the σ -potential indicates the affinity of a component in a mixture towards another. In the σ -potential plot, a higher negative value of μ indicates an increasing interaction between molecules, whereas a more elevated positive value indicates an increase in repulsive behavior. For the horizontal axis, increasing negative and positive values for the hydrogen bonding threshold ($\pm 0.84 \text{ e/nm}^2$) means the region of a molecule where interactions between hydrogen bond donors and hydrogen bond acceptors occur, respectively. The σ -profile and σ -potential of all species involved in this study are depicted in Figs. 6 and 7.

The σ -profile of dibenzofuran has a curve that resolves mostly in the non-polar region. The three significant peaks from the left observed in the dibenzofuran curve correspond to the C–H bonds ($-0.006 \text{ e}\text{\AA}^{-2}$), C atoms with π -electron of the benzene ring ($-0.001 \text{ e}\text{\AA}^{-2}$), and O atom ($0.004 \text{ e}\text{\AA}^{-2}$). The molecular drawing also represents these peaks by the

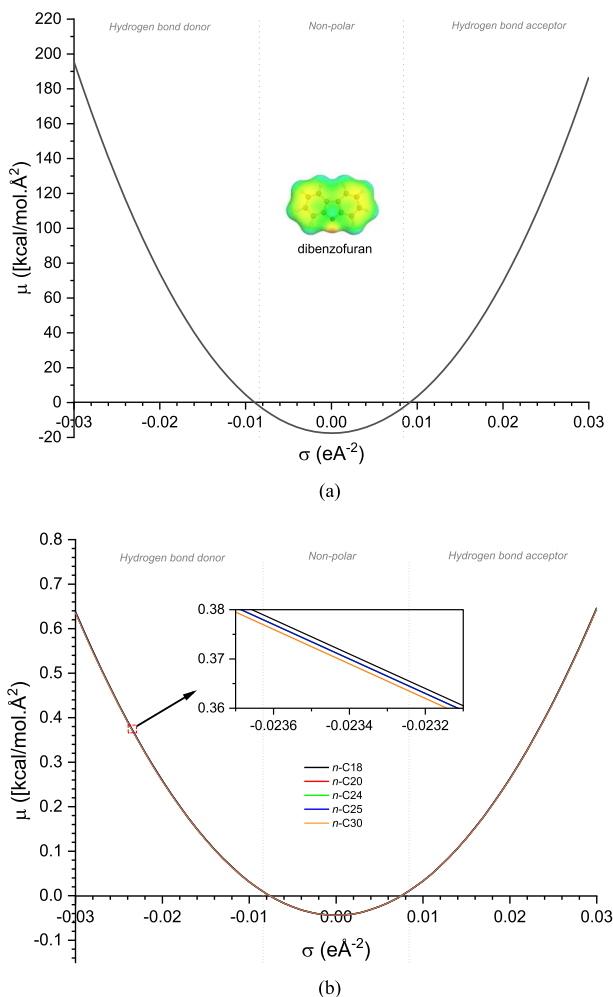
Fig. 6 σ -profiles of dibenzofuran and *n*-alkanes

colors green-cyan, yellow, and orange, respectively. Only a small portion of the dibenzofuran curve falls on the polar regions. On the other hand, the sigma profiles of *n*-alkanes are totally in the non-polar region, with the area under the peak (A) increased proportionally to the carbon number, i.e., $A_{n-C18} < A_{n-C20} < A_{n-C24} < A_{n-C25} < A_{n-C30}$. This can be expected since the addition of carbon number is associated with the increased non-polar charge density of the $-\text{CH}_2$ group.

The polarity and interaction behaviors of dibenzofuran and *n*-alkanes are consistent with the σ -potential depicted in Fig. 7, where the attractive behavior between molecules occurs only in the non-polar region. Although all species showed a similar shape of the curve, dibenzofuran (Fig. 7a) gave a much higher magnitude of repulsive (positive μ) and attractive (negative μ) behavior than those in *n*-alkanes (Fig. 7b). Dibenzofuran has a tiny portion of attractive forces in the polar region. Since dibenzofuran has a relatively higher magnitude of σ -potential than *n*-alkanes, it can be suggested that the increasing molar binary composition of *n*-alkanes (x_2) will have a low impact on reducing the eutectic point. This is in agreement with the curves observed in Fig. 2, where the melting point (T_m) of the binary mixture decreased only slightly at $0.5 \leq x_1 < 1.0$ and reduced rapidly when $x_1 < 0.5$.

COSMO-RS was also able to predict solid–liquid phase equilibria data comparable with, and in some plots, more accurate than other models. For dibenzofuran and *n*-C18 binary mixtures, it can be seen in Fig. 2 that the SLE data points predicted by COSMO-RS gave higher accuracy than those calculated by the UNIFAC and Mod UNIFAC (Dortmund), similar to those of Mod UNIFAC (NIST), and lower than those of Mod UNIFAC (Lyngby). Similarly, in Figs. 3, 4, and 5, COSMO-RS proved its ability to comparably predict the activity coefficients, eutectic compositions, and the eutectic melting temperature of binary mixtures of dibenzofuran and *n*-alkanes. These findings demonstrated the advantage of using COSMO-RS as a predictive tool for calculating thermodynamic properties of mixtures based on molecular information, which requires minimal experimental input. While being an ‘a priori’ method, its inclusion can improve the accuracy of the results by providing additional information about the system. It can also be concluded that COSMO-RS is a valuable tool for predicting the properties of complex mixtures where experimental data may be limited or unavailable, thus offering significant advantages for researchers and practitioners in various fields.

Fig. 7 σ -potentials of **a** dibenzofuran and **b** *n*-alkanes



5 Conclusions

DSC technique is accurate enough to determine the solid–liquid equilibrium data for systems dibenzofuran + *n*-alkanes. Agreement with previous experimental data for pure components was achieved. The method allows the study of the composition effect and the accurate determination of the coordinates for the eutectic point. A linear trend is obtained for the eutectic melting temperature and the eutectic composition versus the alkane number of carbon atoms.

Experimental data show clear non-ideal behavior, verified by predicting the SLE using the ideal solution model. Non-idealities were computed using the group contribution method UNIFAC. Original UNIFAC and several modifications, Mod UNIFAC (Lyngby), Mod UNIFAC (Dortmund), and Mod UNIFAC (NIST), were considered. In general, non-idealities are overestimated, and predicted melting temperatures are higher than experimental values. The best description is obtained with Mod UNIFAC (Lyngby) method, which leads to the lowest deviations in melting temperature and activity coefficients.

A better description is obtained when specific parameters are used. Previously available parameters obtained from data for similar systems lead to lower deviations for melting temperatures and activity coefficients. Data reported here were used to obtain specific parameters for the classical UNIFAC model, and the model's accuracy was improved.

The most recent version of the UNIFAC model, Mod UNIFAC (NIST), includes a specific group for cyclic ethers to define furan compounds. However, such a model version does not improve the results obtained from previous versions. Combining the Mod UNIFAC (Lyngby) with the new group definition (furan group) requires the determination of four binary parameters. Still, the final version leads to an accuracy similar to classical UNIFAC with specific parameters. DISQUAC results are slightly poorer than those obtained from Dortmund UNIFAC with modified interaction parameters.

COSMO-RS was also used in this work to generate the SLE data predictions based on quantum chemical calculations and statistical thermodynamics. The σ -profile and σ -potential developed in COSMO-RS were analyzed to view the behavior of molecular interactions in the binary mixture. This qualitative analysis supported the SLE data points obtained in all calculation models. Prediction from COSMO-RS are similar to UNIFAC (NIST) in spite of COSMO-RS not being a group contribution model.

Supplementary Information The online version contains supplementary material available at <https://doi.org/10.1007/s10953-023-01297-w>.

Acknowledgements Dr. BOUDOUH wishes to express his gratitude to Pr. Juan Antonio González, Professor at the University of Valladolid, Spain, for having welcomed him to the G.E.T.E.F Laboratory. Dr. Hadj-Kali also expresses his appreciation to the Researchers Supporting Project (RSP2023R361), King Saud University, Riyadh, Saudi Arabia.

Author contributions Issam Boudouh: Conceptualization, Investigation, Writing – review & editing, Visualization, Validation. Baudilio Coto: Investigation, Writing – review & editing, Visualization, Software, Data curation, Validation, Supervision. Juan Antonio González: Conceptualization, Investigation, Writing – original draft, Visualization, Software, Data curation, Validation, Supervision. Irfan Wazeer: Investigation, Data curation, Writing – review & editing. M. Zulhaziman M. Salleh: Investigation, Writing – review & editing, Visualization, Software, Data curation, Validation. Ismahane Djemai: Writing – review & editing. Maria Dolores Robustillo: Investigation, Data curation, Writing – review & editing. Mohamed K. Hadj-Kali: Investigation, Writing – review & editing, Visualization, Software, Data curation, Validation.

Declarations

Competing interests The authors declare no competing interests.

References

1. Jennings, D.W., Weispfennig, K.: Experimental solubility data of various n-alkane waxes: effects of alkane chain length, alkane odd versus even carbon number structures, and solvent chemistry on solubility. *Fluid Phase Equilib.* **227**, 27–35 (2005). <https://doi.org/10.1016/j.fluid.2004.10.021>
2. Burger, E., Perkins, T., Striegler, J.: Studies of wax deposition in the trans Alaska pipeline. *J. Petrol. Technol.* **33**, 1075–1086 (1981). <https://doi.org/10.2118/8788-PA>
3. Roenningsen, H.P., Bjoernald, B., Baltzer Hansen, A., Batsberg Pedersen, W.: Wax precipitation from North Sea crude oils: 1. Crystallization and dissolution temperatures, and Newtonian and non-Newtonian flow properties. *Energy Fuels* **5**, 895–908 (1991). <https://doi.org/10.1021/ef00030a019>
4. Coutinho, J.A., Edmonds, B., Moorwood, T., Szczepanski, R., Zhang, X.: Reliable wax predictions for flow assurance. In: European Petroleum Conference, OnePetro, (2002). <https://doi.org/10.2118/78324-MS>

5. Coto, B., Martos, C., Espada, J.J., Robustillo, M.D., Peña, J.L.: Analysis of paraffin precipitation from petroleum mixtures by means of DSC: iterative procedure considering solid–liquid equilibrium equations. *Fuel* **89**, 1087–1094 (2010). <https://doi.org/10.1016/j.fuel.2009.12.010>
6. Hammami, A., Raines, M.: Paraffin deposition from crude oils: comparison of laboratory results with field data. *SPE J.* **4**, 9–18 (1999). <https://doi.org/10.2118/54021-PA>
7. Tuntawiroon, J., Mahidol, C., Navasumrit, P., Autrup, H., Ruchirawat, M.: Increased health risk in Bangkok children exposed to polycyclic aromatic hydrocarbons from traffic-related sources. *Carcinogenesis* **28**, 816–822 (2007). <https://doi.org/10.1093/carcin/bgl1175>
8. Djordjevic, N.: Solubilities of polycyclic aromatic hydrocarbon solids in *n*-octadecane. *Thermochim. Acta* **177**, 109–118 (1991). [https://doi.org/10.1016/0040-6031\(91\)80089-2](https://doi.org/10.1016/0040-6031(91)80089-2)
9. Aoulmi, A., Bouroukba, M., Solimando, R., Rogalski, M.: Thermodynamics of mixtures formed by polycyclic aromatic hydrocarbons with long chain alkanes. *Fluid Phase Equilib.* **110**, 283–297 (1995). [https://doi.org/10.1016/0378-3812\(95\)02759-8](https://doi.org/10.1016/0378-3812(95)02759-8)
10. Mahmoud, R., Solimando, R., Bouroukba, M., Rogalski, M.: Solid–liquid equilibrium and excess enthalpy measurements in binary dibenzofuran or xanthene+normal long-chain alkane systems. *J. Chem. Eng. Data* **45**, 433–436 (2000). <https://doi.org/10.1021/je9902084>
11. Hafsaoui, S., Mahmoud, R.: Solid-liquid equilibria of binary systems containing *n*-tetracosane with naphthalene or dibenzofuran: prediction with UNIFAC model. *J. Therm. Anal. Calorim.* **88**, 565–570 (2007). <https://doi.org/10.1007/s10973-006-8084-2>
12. Burley, S., Petsko, G.: Weakly polar interactions in proteins. *Adv. Protein Chem.* **39**, 125–189 (1988). [https://doi.org/10.1016/S0065-3233\(08\)60376-9](https://doi.org/10.1016/S0065-3233(08)60376-9)
13. Mahmoud, R., Solimando, R., Rogalski, M.: Solid–liquid equilibria of systems containing pyrene and long chain normal-alkanes. *Fluid Phase Equilib.* **148**, 139–146 (1998). [https://doi.org/10.1016/S0378-3812\(98\)00204-0](https://doi.org/10.1016/S0378-3812(98)00204-0)
14. Boudouh, I., Djemai, I., González, J.A., Barkat, D.: Solid–liquid equilibria of biphenyl binary systems. *J. Mol. Liq.* **216**, 764–770 (2016). <https://doi.org/10.1016/j.molliq.2016.02.010>
15. Boudouh, I., Hafsaoui, S.L., Mahmoud, R., Barkat, D.: Measurement and prediction of solid–liquid phase equilibria for systems containing biphenyl in binary solution with long-chain *n*-alkanes. *J. Therm. Anal. Calorim.* **125**, 793–801 (2016). <https://doi.org/10.1007/s10973-016-5407-9>
16. Boudouh, I., Barkat, D., González, J.A., Djemai, I.: Solid-liquid equilibria of indole binary systems. *Thermochim. Acta* **644**, 13–19 (2016). <https://doi.org/10.1016/j.tca.2016.10.003>
17. Boudouh, I., González, J.A., Djemai, I., Barkat, D.: Solid-liquid equilibria of eicosane, tetracosane or biphenyl + 1-octadecanol, or + 1-eicosanol mixtures. *Fluid Phase Equilib.* **442**, 28–37 (2017). <https://doi.org/10.1016/j.fluid.2017.03.012>
18. Boudouh, I., González, J.A., Coto, B., Moussaoui, A., Kasmi, A., Djemai, I., Hadj-Kali, M.K.: Solid-liquid equilibria for dibenzofuran or Xanthene + heavy hydrocarbons: Experimental measurements and modeling. *J. Mol. Liq.* **116536**, 335 (2021). <https://doi.org/10.1016/j.molliq.2021.116536>
19. Boudouh, I., Tamura, K., Djemai, I., Robustillo-Fuentes, M.D., Hadj-Kali, M.K.: Solid-liquid equilibria for biphenyl+ *n*-tetracosane binary mixtures and *n*-tetracosane+ dibenzofuran+ biphenyl ternary mixtures: experimental data and prediction with UNIFAC models. *Int. J. Thermophys.* **43**, 1–18 (2022). <https://doi.org/10.1007/s10765-022-03025-w>
20. Hansen, H.K., Rasmussen, P., Fredenslund, A., Schiller, M., Gmehling, J.: Vapor–liquid equilibria by UNIFAC group contribution. 5. Revision and extension. *Ind. Eng. Chem. Res.* **30**, 2352–2355 (1991). <https://doi.org/10.1021/ie00058a017>
21. Weidlich, U., Gmehling, J.: A modified UNIFAC model. 1. Prediction of VLE, h^E , and γ^∞ . *Ind. Eng. Chem. Res.* **26**, 1372–1381 (1987). <https://doi.org/10.1021/ie00067a018>
22. Gmehling, J., Li, J., Schiller, M.: A modified UNIFAC model. 2. Present parameter matrix and results for different thermodynamic properties. *Ind. Eng. Chem. Res.* **32**, 178–193 (1993). <https://doi.org/10.1021/ie00013a024>
23. Fredenslund, A., Jones, R.L., Prausnitz, J.M.: Group-contribution estimation of activity coefficients in nonideal liquid mixtures. *AIChE J.* **21**, 1086–1099 (1975)
24. Larsen, B.L., Rasmussen, P., Fredenslund, A.: A modified UNIFAC group-contribution model for prediction of phase equilibria and heats of mixing. *Ind. Eng. Chem. Res.* **26**, 2274–2286 (1987). <https://doi.org/10.1021/ie00071a018>
25. Kang, J.W., Diky, V., Frenkel, M.: New modified UNIFAC parameters using critically evaluated phase equilibrium data. *Fluid Phase Equilib.* **388**, 128–141 (2015). <https://doi.org/10.1016/j.fluid.2014.12.042>
26. Kehiaian, H.V.: Group contribution methods for liquid mixtures: A critical review. *Fluid Phase Equilib.* **13**, 243–252 (1983). [https://doi.org/10.1016/0378-3812\(83\)80098-3](https://doi.org/10.1016/0378-3812(83)80098-3)

27. Klamt, A.: Conductor-like screening model for real solvents: a new approach to the quantitative calculation of solvation phenomena. *J. Phys. Chem.* **99**, 2224–2235 (1995)
28. Prausnitz, J.M., Lichtenthaler, R.N., De Azevedo, E.G.: *Molecular Thermodynamics of Fluid Phase Equilibria*. Pearson Education, New Jersey (1998)
29. Guggenheim, E.A.: *Mixtures*. Oxford University Press, Oxford (1952)
30. Bondi, A.A.: *Physical properties of Molecular Crystals Liquids, and Glasses*. Wiley, New York (1968)
31. Kehiaian, H.V., Grolier, J.P.E., Benson, G.C.: Thermodynamics of organic mixtures. A generalized quasichemical theory in terms of group surface interactions. *J. Chim. Phys.* **75**, 1031–1048 (1978). <https://doi.org/10.1051/jcp/1978751031>
32. González, J., de la Fuente, I.G., Cobos, J., Casanova, C., Ait-Kaci, A.: Application of the zeroth approximation of the DISQUAC model to cyclohexane+ *n*-alkane mixtures using different combinatorial entropy terms. *Fluid Phase Equilib.* **112**, 63–87 (1995). [https://doi.org/10.1016/0378-3812\(95\)02783-B](https://doi.org/10.1016/0378-3812(95)02783-B)
33. González, J.A., de la Fuentá, I.G., Cobos, J.C.: Thermodynamics of mixtures with strongly negative deviations from Raoult's Law: Part 4. Application of the DISQUAC model to mixtures of 1-alkanols with primary or secondary linear amines. Comparison with Dortmund UNIFAC and ERAS results. *Fluid Phase Equilib.* **168**, 31–58 (2000). [https://doi.org/10.1016/S0378-3812\(99\)00326-X](https://doi.org/10.1016/S0378-3812(99)00326-X)
34. González, J.A., Zawadzki, M., Domanska, U.: Thermodynamics of mixtures containing polycyclic aromatic hydrocarbons. *J. Mol. Liq.* **143**, 134–140 (2008). <https://doi.org/10.1016/j.molliq.2008.07.005>
35. Marongiu, B., Piras, A., Porcedda, S., Tuveri, E.: Excess enthalpies of aromatic ether or aromatic ketone (1)+ *n*-heptane (2) mixtures DISQUAC analysis. *J. Therm. Anal. Calorim.* **92**, 137–144 (2008). <https://doi.org/10.1007/s10973-007-8752-x>
36. Klamt, A., Jonas, V., Bürger, T., Lohrenz, J.C.: Refinement and parametrization of COSMO-RS. *J. Phys. Chem. A* **102**, 5074–5085 (1998)
37. Klamt, A., Eckert, F.: COSMO-RS: a novel and efficient method for the a priori prediction of thermophysical data of liquids. *Fluid Phase Equilib.* **172**, 43–72 (2000). [https://doi.org/10.1016/S0378-3812\(00\)00357-5](https://doi.org/10.1016/S0378-3812(00)00357-5)
38. Klamt, A.: *COSMO-RS: from Quantum Chemistry to Fluid Phase Thermodynamics and Drug Design*. Elsevier, Amsterdam (2005)
39. Eckert, F., Klamt, A.: Fast solvent screening via quantum chemistry: COSMO-RS approach. *AICHE J.* **48**, 369–385 (2002). <https://doi.org/10.1002/aic.690480220>
40. Kniáz, K.: Influence of size and shape effects on the solubility of hydrocarbons: the role of the combinatorial entropy. *Fluid Phase Equilib.* **68**, 35–46 (1991). [https://doi.org/10.1016/0378-3812\(91\)85009-J](https://doi.org/10.1016/0378-3812(91)85009-J)
41. Khimeche, K., Boumrah, Y., Benziane, M., Dahmani, A.: Solid–liquid equilibria and purity determination for binary *n*-alkane + naphthalene systems. *Thermochim. Acta* **444**, 166–172 (2006). <https://doi.org/10.1016/j.tca.2006.03.011>
42. Benziane, M., Khimeche, K., Dahmani, A., Nezar, S., Trache, D.: Experimental determination and prediction of (solid+ liquid) phase equilibria for binary mixtures of heavy alkanes and fatty acids. *Mol. Phys.* **110**, 1383–1389 (2012). <https://doi.org/10.1007/s10973-012-2654-2>
43. Company, J.C.: Mésure et interprétation des équilibres de cristallisation de solutions de paraffines lourdes et d'hydrocarbures aromatiques. *Chem. Eng. Sci.* **28**, 318–323 (1973). [https://doi.org/10.1016/0009-2509\(73\)85117-6](https://doi.org/10.1016/0009-2509(73)85117-6)
44. Mondieig, D., Rajabalee, F., Metivaud, V., Oonk, H., Cuevas-Diarte, M.: *n*-Alkane binary molecular alloys. *Chem. Mater.* **16**, 786–798 (2004). <https://doi.org/10.1021/cm031169p>

Publisher's Note Springer Nature remains neutral with regard to jurisdictional claims in published maps and institutional affiliations.

Springer Nature or its licensor (e.g. a society or other partner) holds exclusive rights to this article under a publishing agreement with the author(s) or other rightsholder(s); author self-archiving of the accepted manuscript version of this article is solely governed by the terms of such publishing agreement and applicable law.

Authors and Affiliations

Issam Boudouh^{1,2} · Baudilio Coto³ · Juan Antonio González⁴ · Irfan Wazeer⁵ · M. Zulhaziman M. Salleh⁶ · Ismahane Djemai⁷ · Maria Dolores Robustillo⁸ · Mohamed K. Hadj-Kali⁵

✉ Issam Boudouh
issam-boudouh@univ-eloued.dz

¹ Département de Génie des Procédés et Péetrochimie, Université Echahid Hamma Lakhdar, BP 789, 39000 El Oued, Algeria

² Département de Génie des Procédés, Faculté de Technologie, Université de Batna 2, 53, Route de Constantine, Fésdis, 05078 Batna, Algeria

³ Department of Chemical and Energy Technology, ESCET, Universidad Rey Juan Carlos, C/Tulipán s/n, 28933 Móstoles, Madrid, Spain

⁴ G.E.T.E.F., Grupo Especializado en Termodinámica de Equilibrio Entre Fases, Departamento de Física Aplicada, Facultad de Ciencias, Universidad de Valladolid, 47071 Valladolid, Spain

⁵ Chemical Engineering Department, College of Engineering, King Saud University, PO Box 800, Riyadh 11421, Saudi Arabia

⁶ Department of Chemical and Process Engineering, Faculty of Engineering and Built Environment, Universiti Kebangsaan Malaysia, 43600 Bangi, Selangor, Malaysia

⁷ Département d'Hydraulique, Université de Batna 2, 53, Route de Constantine, Fésdis, 05078 Batna, Algeria

⁸ Department of Chemical and Environmental Engineering, Universidad Politécnica de Madrid, José Gutiérrez Abascal 2, 28006 Madrid, Spain